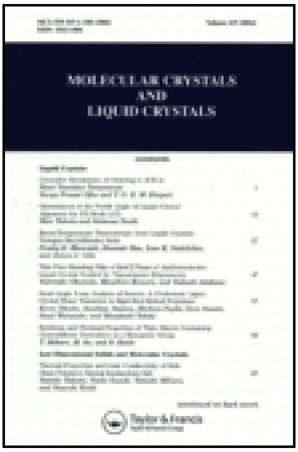

Molecular Crystals and Liquid Crystals
Publication details, including instructions for authors and subscription information:
http://www.tandfonline.com/loi/gmcl20

Synthesis, Characterization and Mesomorphic Properties of Aromatic Acid Dimers

Ashwini Pandey [a] & Bachcha Singh [a]

[a] Department of Chemistry (Centre of Advanced Study), Faculty of Science, Banaras Hindu University, Varanasi, India

To cite this article: Ashwini Pandey & Bachcha Singh (2012): Synthesis, Characterization and Mesomorphic Properties of Aromatic Acid Dimers, Molecular Crystals and Liquid Crystals, 552:1, 43-52

To link to this article: http://dx.doi.org/10.1080/15421406.2011.599215

Mol. Cryst. Liq. Cryst., Vol. 552: pp. 43–52, 2012

ISSN: 1542-1406 print/1563-5287 online
DOI: 10.1080/15421406.2011.599215

Synthesis, Characterization and Mesomorphic Properties of Aromatic Acid Dimers

ASHWINI PANDEY AND BACHCHA SINGH*

Department of Chemistry (Centre of Advanced Study), Faculty of Science,
Banaras Hindu University, Varanasi, India

In this study, a new series of acid dimers, N-(4′-carboxybenzylidene)-4-alkoxybenzoyloxyaniline [(4′-$HOOCC_6H_4CH{=}N$)-4-$C_6H_4OCOC_6H_4OR$, where $R = C_mH_{2m+1}$ and $m = 6, 8, 10, 12, 14$, and 16], have been synthesized. The compounds have been characterized by elemental analyses and FTIR, UV-visible, ^1H, and ^{13}C NMR spectra. The mesomorphic properties of these acid dimers were studied by differential scanning calorimetry and polarizing optical microscopy. The mesomorphic nature of these compounds depends on hydrogen bonding and on the alkoxy chain length. The compounds with $m = 6$ and 8 show a characteristic enantiotropic nematic mesophase, whereas those with $m = 12$ and 14 exhibit monotropic behavior. The compounds with $m = 10$ and 16 exhibit non-mesomorphic behavior.

Keywords Differential scanning calorimetry; enantiotropic nematic mesophase; monotropic nematic mesophase; polarizing optical microscopy; acid dimers

1. Introduction

Supermolecular liquid crystals (LCs) obtained via intermolecular hydrogen bonding have attracted considerable attention during the last decade [1–21]. Although the first report of hydrogen bonding in liquid crystals dates back to the 1960s [22,23], much research took place in the last two decades of the twentieth century [2,6,9,24–28]. New molecular shapes, self-assembled structures, and unexpected properties have been found in liquid crystalline materials. A variety of functional groups can be introduced as a part of mesogenic components in these self-assembled materials. These new exotic liquid crystalline materials have attracted considerable attention because of their great potential for new dynamic functions, such as ion, charge, and mass transportation; photo-function; sensing; stimuli-responsive properties; and bio-function [29,30].

In 1989, Kato and Fréchet found that 1:1 complexation of benzoic acid and stilbazole leads to the formation of a well-defined structure of a hydrogen-bonded mesogen by intermolecular hydrogen bonding between the carboxylic acid and the pyridine [2].

Lehn et al. found that diaminopyridines and uracil derivatives form triply hydrogen-bonded liquid crystalline complexes [31]; they also form columnar liquid crystalline structures. These early studies by Kato and Fréchet [1,2] and Lehn et al. [31,32] have shown great importance of the use of hydrogen bonding not only in the design of liquid crystals but also

---

*Address correspondence to Bachcha Singh, Department of Chemistry (Centre of Advanced Study), Faculty of Science, Banaras Hindu University, Varanasi 221005, India. E-mail: bsinghbhu@rediffmail.com in the design of condensed states of soft materials, such as polymers, low-molecular-weight organic molecules, and composites.

Many reports in the current literature involve the formation of LCs through the hydrogen bonding of aromatic carboxylic acids, as well as from mixtures of unlike molecules capable of interacting through hydrogen bonding [17,21,24,28–40].

The occurrence of hydrogen bonding in LCs, often referred to as the fifth fundamental type of interaction, is considered to be the basis for the origin of new stable mesophases, with a wide thermal stability. It has been well established [21] that the formation of hydrogen bonding in liquid crystalline materials can be tuned, through the proper selection of complementary interacting components, to fix the configuration (with respect to the direction of the LC rigid core) of the hydrogen bonds formed.

Owing to the abovementioned properties of the hydrogen-bonded LCs, it was thought worthwhile to synthesize a series of hydrogen-bonded compounds having ester and aldimine linkages with terminal carboxyl group which undergoes dimerization in the presence of N,N-dimethyl formamide. These series of compounds, namely, N-(4′-carboxybenzylidene)-4-alkoxybenzoyloxyaniline, with $m = 6{\sim}16$, have been synthesized and characterized on the basis of IR, NMR (^{1}H and ^{13}C) and UV-visible spectroscopy. The mesomorphic properties have been investigated by polarizing optical microscopy (POM) and differential scanning calorimetry (DSC). The details of the synthesis and characterization of these compounds have been described in the present paper.

2. Experimental Details

2.1 Materials

4-Formyl benzoic acid, 4-hydroxybenzoic acid, 1-bromoalkane, 4-aminophenol, and potassium hydroxide purchased from Aldrich Chemicals, USA, were used as received. Reagent-grade solvents and reactants were purchased commercially and used after purification.

2.2 Techniques

Elemental analyses were performed on a CE-440 Exeter analytical CHN (carbon, hydrogen, nitrogen) analyzer. IR spectra were recorded on an FTIR Varian 3100 Excalibur series spectrophotometer in KBr pellet in the 4000–100 cm^{-1} region. ^{1}H and ^{13}C NMR spectra were obtained on a JEOL FT-NMR AL 300 MHz spectrometer using tetramethyl silane as the internal standard. Electronic spectra were recorded on a UV-1700 Pharma Spec Shimadzu UV-visible spectrophotometer. DSC thermograms were recorded with a Mettler Toledo TC 15 TA DSC at a rate of 10.0 K min^{-1} under a nitrogen atmosphere using special pure grade zinc and indium as standards by taking samples in close-lid aluminum pans. The transition temperatures from DSC have been determined with an accuracy of ± 0.1K. The mesophase type of compounds were identified by visual comparison with known phase standards using an HT 30.01 NTT 268 Lomo POM fitted with a hot stage with temperature controlling accuracy of 0.1 K.

2.3 Synthesis of Compounds

4-n-Alkoxybenzoic acids (**2**), namely 4-hexyloxy-, 4-octyloxy-, 4-decyloxy-, 4-dodecyloxy-, 4-tetradecyloxy-, and 4-hexadecyloxybenzoic acids, were synthesized by the method described elsewhere [41].

*2.3.1 4-n-alkoxybenzoyl chlorides (**3**).* These were prepared from the corresponding acids [42].

*2.3.2 4-[(4′-carboxy)benzylidene]aminophenol (**6**).* 4-Aminophenol (**4**) (1.09 g, 10 mmol) and 4-formylbenzoic acid (**5**) (1.5 g, 10 mmol) were mixed in ethanol (20 ml), followed by addition of 2–3 drops of glacial acetic acid, and refluxed for 4 h. The reaction mixture became dark yellow. The solvent was evaporated under reduced pressure to yield a yellow residue, which was washed 2–3 times with distilled water, dried, and recrystallized from chloroform with a 65% yield. FTIR (KBr, cm^{-1}): 3588 (OH phenolic), 3308 (OH acid), 2997, 1687 (C=O acid), 1617 (C=N), 1583, 1504 (Ph), 1422, 1374, 1289, 1241, 1167 cm^{-1}. ^{1}H NMR (DMSO, TMS) δ (ppm): 9.63 (s, 1H, —OH), 8.70 (s, 1H, —CH=N), 8.05–6.80 (m, 8H, ArH). ^{13}C NMR δ_c (DMSO): 167.1, 156.8, 156.0, 142.1, 140.1, 132.6, 129.7, 128.2, 122.8, 115.8, 48.6, 40.3, 39.7, 39.5, 39.2, 38.9, 38.6. UV-visible (DMF): λ_{max} = 394, 353, 300, 243 nm. Elemental analyses: calculated for $C_{14}H_{11}NO_3$, (%), C, 69.73; H, 4.59; N, 5.80; Found C, 69.54; H, 4.81; N, 5.49.

*2.3.3 N-(4′-carboxybenzylidene)-4-hexyloxybenzoyloxyaniline (**7a**).* To a solution of 4-n-hexyloxybenzoyl chloride (1.20 g, 5 mmol) in DMF (50 ml) was added 1.20 g (5 mmol) of 4-[(4′-carboxy)benzylidene]aminophenol (**6**) along with the addition of 2–3 drops of pyridine, resulting in a yellow solution. The soultion was heated at 80°C for 9 h when the color changed from yellow to reddish brown. The reaction mixture was cooled to room temperature and 50 ml of distilled water was added. The solution was agitated and the product was extracted with 2 × 50 ml of chloroform. The chloroform extract was dried over magnesium sulfate (anhydrous), filtered, and recrystallized from chloroform after concentration. The reddish-brown crystals of N-(4′-carboxybenzylidene)-4-hexyloxybenzoyloxyaniline were obtained in a 61% yield. FTIR (KBr, cm^{-1}): 3423, 2931, 2856 (aliphatic C—H), 2558 (OH dimer), 1776 (C=O ester), 1688 (C=O dimer acid), 1606 (Ph), 1511 (C=N), 1466, 1428, 1390 (C—O—H), 1298 (C—O ester), 1166, 1066, 993, 935 (out-of-plane OH bend), 843,769. ^{1}H NMR (DMSO) δ_H (ppm): 12.56 (s, 1H, —OH), 9.82 (s, 1H, —CH=N), 7.86–6.95 (m, 12H, ArH), 4.02–3.98 (t, 2H, $-OCH_2$), 1.72–1.24 (m, 8H, $-[CH_2]_n$), 0.92–0.82 (t, 3H, $-CH_3$). ^{13}C NMR ($CDCl_3$) δ_c ($CDCl_3$): 171.9, 163.6, 132.3, 129.5, 127.1, 121.3, 116.3, 114.1, 77.4, 77.0, 76.5 ($CDCl_3$), 68.2 ($-OCH_2$), 31.5, 29.6, 29.0, 25.6, 22.5, 14.0 (CH_3). UV-visible ($CHCl_3$): λ_{max} = 301, 264 nm. Elemental analyses: calculated for $C_{27}H_{27}NO_5$ (%), C, 72.79; H, 6.10; N, 3.14; Found C, 72.58; H, 5.94; N, 3.11.

All other members of the homologous series, namely N-(4′-carboxybenzylidene)-4-octyloxy-, 4-decyloxy-, 4-dodecyloxy-, 4-tetradecyloxy-, and 4-hexadecyloxybenzoylo xyanilines, were prepared by following the above procedure.

*2.3.4 N-(4′-carboxybenzylidene)-4-octyloxybenzoyloxyaniline (**7b**).* Yield: 67%. FTIR (KBr, cm^{-1}): 3421, 2928, 2854 (aliphatic C—H), 2554 (OH), 1774 (C=O), 1687 (C=O dimer acid), 1605 (Ph), 1511 (C=N), 1464, 1428, 1391 (C—O—H bend), 1298 (C—O ester), 1162, 1064, 991, 932 (out-of-plane OH bend), 843, 768. ^{1}H NMR ($CDCl_3$, TMS) δ_H (ppm): 12.56 (s, 1H, —CH=N), 7.99–6.87 (m, 12H, ArH), 4.37–3.97 (t, 2H, $-OCH_2$), 1.81–1.25 (m, 12H, $-[CH_2]_n$), 0.93–0.88 (t, 3H, $-CH_3$). ^{13}C NMR δ_c ($CDCl_3$): 171.8, 163.6, 132.3, 129.5, 127.1, 121.3, 116.3, 114.0, 77.4, 77.0, 76.5 ($CDCl_3$), 68.2 ($-OCH_2$), 31.5, 29.6, 29.0, 25.6, 22.5, 14.0 (CH_3). UV-visible ($CHCl_3$): λ_{max} = 289, 256, 213 nm. Elemental analyses: calculated for $C_{29}H_{31}NO_5$ (%), C, 73.55; H, 6.59; N, 2.95; Found C, 73.41; H, 6.28; N, 2.56.

*2.3.5 N-(4′-carboxybenzylidene)-4-decyloxybenzoyloxyaniline (**7c**).* Yield: 62%. FTIR (KBr, cm^{-1}): 3420, 2928, 2854 (aliphatic C—H), 2550 (OH), 1773 (C=O), 1680 (C=O dimer acid), 1606 (Ph), 1510 (C=N), 1464, 1428, 1391 (C—O—H bend), 1298 (C—O ester), 1162, 1064, 991, 932 (out-of-plane OH bend), 843, 769. ^{1}H NMR ($CDCl_3$, TMS) δ_H (ppm) 12.56 (s, 1H, OH), 9.82 (s, 1H, —CH=N), 7.99–6.87 (m, 12H, ArH), 4.37–3.97 (t, 2H, —OCH_2), 1.81–1.25 (m, 16H, —$[CH_2]_n$), 0.93–0.88 (t, 3H, —CH_3).^{13}C NMR δ_c ($CDCl_3$): 171.9, 163.4, 132.2, 129.5, 127.1, 121.2, 116.3, 114.0, 77.4, 77.0, 76.5 ($CDCl_3$), 68.2 (—OCH_2), 31.5, 29.6, 29.0, 25.6, 22.5, 14.0 (CH_3). UV-visible ($CHCl_3$): λ_{max} = 357, 270, 252, 212 nm. Elemental analyses: calculated for $C_{31}H_{35}NO_5$ (%), C, 74.22; H, 7.03; N, 2.79; Found C, 73.81; H, 7.11; N, 2.64.

*2.3.6 N-(4′-carboxybenzylidene)-4-dodecyloxybenzoyloxyaniline (**7d**).* Yield: 58%. FTIR (KBr, cm^{-1}): 3431, 2922, 2852 (aliphatic C—H), 2557 (OH), 1774 (C=O), 1684 (C=O dimer acid), 1606 (Ph), 1513 (C=N), 1464, 1430, 1390 (C—O—H bend), 1307 (C—O ester), 1170, 1061, 991, 935 (out-of-plane OH bend), 845, 770. ^{1}H NMR ($CDCl_3$, TMS) δ_H (ppm) 12.52 (s, 1H, OH), 9.82 (s, 1H, —CH=N), 8.05–6.91 (m, 12H, ArH), 4.04–3.97 (t, 2H, —OCH_2), 1.82-1.26 (m, 20H, —$[CH_2]_n$), 0.87 (t, 3H, —CH_3).^{13}C NMR δ_c ($CDCl_3$): 171.9, 163.6, 132.3, 129.5, 127.5, 121.2, 116.3, 114.0, 77.4, 77.0, 76.5 ($CDCl_3$), 68.2 (—OCH_2), 31.7, 29.5, 25.6, 22.5, 14.0 (CH_3). UV-visible ($CHCl_3$): λ_{max} = 279, 264, 253, 228, 213 nm. Elemental analyses: calculated for $C_{33}H_{39}NO_5$ (%), C, 74.83; H, 7.42; N, 2.64; Found C, 74.56; H, 7.08; N, 2.36.

*2.3.7 N-(4′-carboxybenzylidene)-4-tetradecyloxybenzoyloxyaniline (**7e**).* Yield: 55%. FTIR (KBr, cm^{-1}): 3450, 2918, 2851 (aliphatic C—H), 2562 (OH), 1778 (C=O), 1684 (C=O dimer acid), 1607 (Ph), 1513 (C=N), 1469, 1429, 1392 (C—O—H bend), 1304 (C—O ester), 1171, 1061, 992, 941 (out-of-plane OH bend), 846, 718. ^{1}H NMR ($CDCl_3$, TMS) δ_H (ppm) 12.56 (s, 1H, OH), 9.82 (s, 1H, —CH=N), 7.86–6.95 (m, 12H, ArH), 4.02–3.98 (t, 2H, —OCH_2), 1.72–1.24 (m, 24H, -$[CH_2]_n$), 0.92–0.82 (t, 3H, —CH_3). ^{13}C NMR δ_c ($CDCl_3$): 171.9, 163.6, 132.3, 129.4, 127.5, 121.1, 116.3, 114.1, 77.4, 77.0, 76.5 ($CDCl_3$), 68.2 (—OCH_2), 31.7, 29.5, 29.0, 25.6, 22.5, 14.0 (CH_3). UV-visible ($CHCl_3$): λ_{max} = 279, 227, 213 nm. Elemental analyses: calculated for $C_{35}H_{43}NO_5$ (%), C, 75.37; H, 7.77; N, 2.51; Found C, 75.12; H, 7.54; N, 2.38.

*2.3.8 N-(4′-carboxybenzylidene)-4-hexadecyloxybenzoyloxyaniline (**7f**).* Yield: 58%. FTIR (KBr, cm^{-1}): 3452, 2922, 2855 (aliphatic C—H), 2559 (OH), 1775 (C=O), 1688 (C=O dimer acid), 1605 (Ph), 1515 (C=N), 1469, 1431, 1390 (C—O—H bend), 1305 (C—O ester), 1172, 1058, 991, 925 (out-of-plane OH bend), 841, 714. ^{1}H NMR ($CDCl_3$, TMS) δ_H (ppm): 12.52 (s, 1H, OH), 9.82 (s, 1H, —CH=N), 7.86–6.95 (m, 12H, ArH), 4.02–3.98 (t, 2H, —OCH_2), 1.72–1.24 (m, 28H, —$[CH_2]_n$), 0.92-0.82 (t, 3H, —CH_3). ^{13}C NMR δ_c ($CDCl_3$): 171.9, 163.6, 132.2, 129.3, 127.5, 121.1, 116.4, 114.1, 77.4, 77.0, 76.5 ($CDCl_3$), 68.2 (—OCH_2), 31.7, 29.5, 29.0, 25.6, 22.5, 14.0 (CH_3). UV-visible ($CHCl_3$): λ_{max} = 280, 230, 210 nm. Elemental analyses: calculated for $C_{37}H_{47}NO_5$ (%), C, 75.86; H, 8.08; N, 2.39; Found C, 75.52; H, 7.92; N, 2.14.

3. Results and Discussion

The synthetic route for the compounds 4-[(4′-carboxy)benzylidene] aminophenol (**6**) and its ester derivative N-(4′-carboxybenzylidene)-4-alkoxybenzoyloxyaniline (**7**) is outlined in Scheme 1. The elemental analyses, FTIR, and NMR spectra are fully consistent with

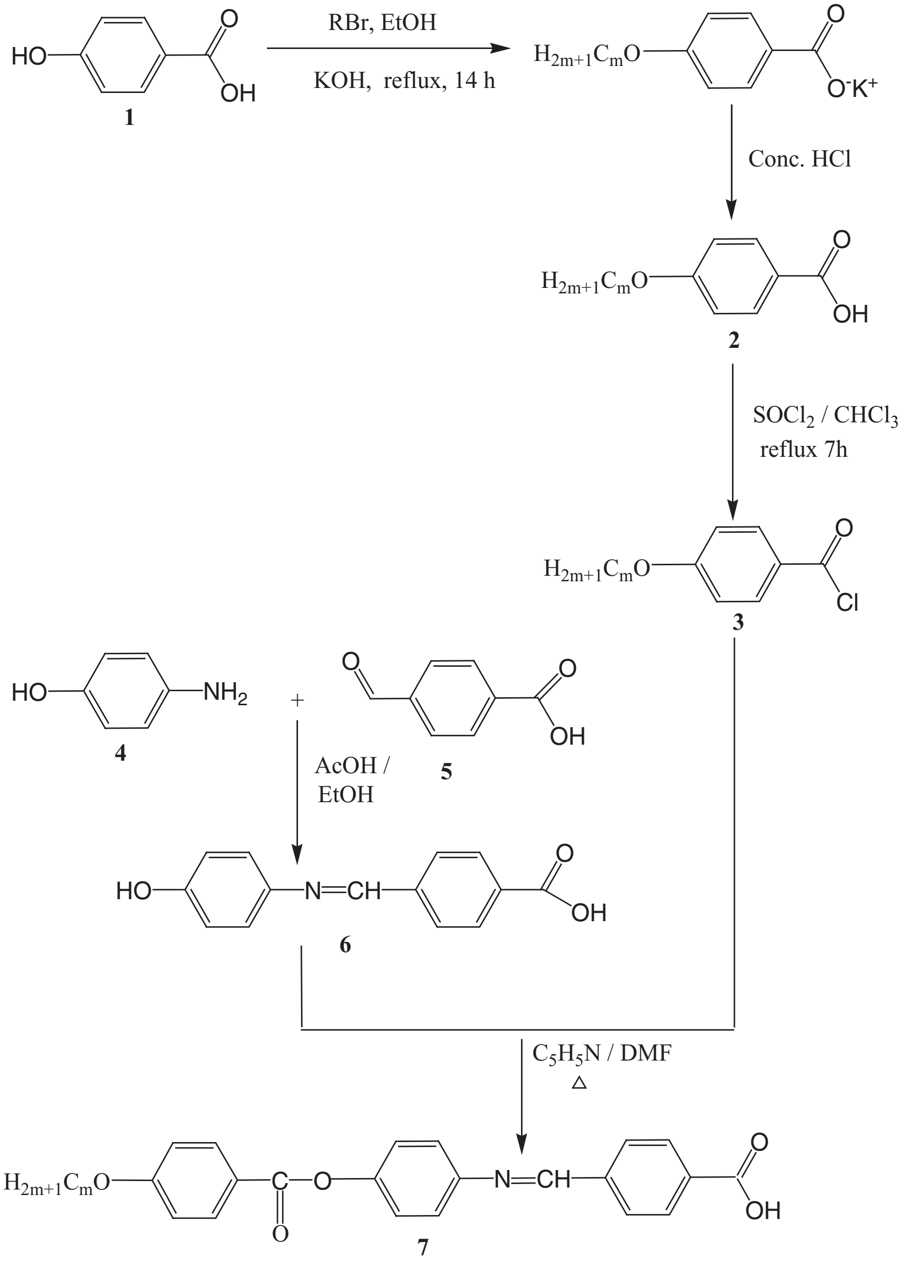

Scheme 1. Route for the synthesis of N-(4′-carboxybenzylidene)-4-alkoxybenzyoyloxyaniline.

the structure. The IR spectrum of 4-[(4′-carboxy)benzylidene]aminophenol (**6**) exhibits major bands at 3588 , 3308, 2997, 1687, 1617, 1583, and 1504 cm^{-1}, which are characteristic of ν(OH phenolic), ν(OH acid), aromatic C—H, ν(C=N), and ring C—C stretch, respectively. The compound undergoes esterification with 4-n-hexyloxybenzoyl chloride in the presence of pyridine to form N-(4′-carboxybenzylidene)-4-hexyloxybenzoyloxyaniline

(**7**). This compound exhibits IR bands at 3423, 2931, 2856, 2558, 1776, 1688, 1606, 1511, 1390, and 1298 cm^{-1}, which are attributed to ν(OH) acid, ν(aliphatic C—H), ν(OH) dimer acid, ν(COO ester), ν(C=O dimer acid), ν(Ph), ν(C=N), ν(C—O—H bending mode), and ν(C—O ester). Further, a characteristic band for the dimeric carboxylic acid resulting from the out-of-plane bending of the bonded O—H appears near 935 cm^{-1}.

The dimer state of this compound formed as a result of intermolecular hydrogen bonding depicts major hydrogen bonding peaks centered at 2856, 1688, and 935 cm^{-1} assigned to ν(OH dimer acid) and ν(C=O) dimer acid, and an exclusive band for OH out-of-plane bending mode characteristic of the dimeric acid appears at 935 cm^{-1}. Comparison of the dimeric hydrogen-bonded peaks with the non-hydrogen-bonded peaks for the same compound depicts a major or a significant shift in the C=O for the non-hydrogen-bonded acid appearing at 1714 cm^{-1} to 1688 cm^{-1} in the hydrogen-bonded compound along with the appearance of a new band for out-of-plane OH bending at 935 cm^{-1}, which is absent in non-hydrogen-bonded compound.

The ^{1}H NMR spectrum of 4-[(4′-carboxy)benzylidene]aminophenol (**6**) exhibits signals at δ 9.63 (s), 8.70 (s), and 8.05–6.80 (m), which are attributed to —OH, —CH=N, and aromatic ring protons, respectively. The major signals in the ^{13}C NMR spectrum of the compound (**6**) are observed at δ 167.1 for —CH=N, 156.8 for C—OH, 142.1 for carbon of aromatic ring bonded to N of CH=N, and the one centered at 132.6 is assigned for the aromatic ring carbon. The signals appearing for ^{1}H and ^{13} C NMR are fully consistent with the structure. Furthermore, the proton NMR of the compound of N-(4′-carboxybenzylidene)-4-hexyloxybenzoyloxyaniline (**7a**) exhibits sharp signals at δ 12.56 (s), 9.82 (s), 7.99–6.87 (m), 4.37–3.97 (t), 1.81–1.25 (m), and 0.93–0.88 are attributed to —OH, —CH=N, aromatic ring, $—OCH_2$, $—[CH_2]_n$, and CH_3 protons, respectively. The ^{13}C NMR signals for the major functional groups for this compound are observed at δ 171.9 for $\underline{C}OOH$ attached to aromatic ring, 163.6 for $—\underline{C}H{=}N$, 132.3, 129.5 for carbons of aromatic ring, 77.4, 77.0, 77.5 for $CDCl_3$, and the ones centered at 68.2, 25.6, and 14.0 are attributed for $—O\underline{C}H_2$, $—OCH_2\underline{C}H_2$, and CH_3 carbon signals, suggesting the consistency of the signals with the molecular structure.

The electronic spectrum of the compound N-(4′-carboxybenzylidene)-4-hexyloxybenzoyloxyaniline (**7a**) display UV bands at 289, 256, and 213 nm, which are assigned for n-π^*, B-band of benzene, and π–π^* transitions.

All other members of the homologous series with intermolecular hydrogen-bonding-generating acid dimers exhibit similar IR, NMR, and UV-visible bands, which are already explained and their structures have been elucidated on the basis of the abovementioned analytical techniques.

4. Optical Properties

The liquid crystalline properties of N-(4′-carboxybenzylidene)-4-n-alkoxybenzoyl oxyaniline **7a–7f** were investigated by POM using a heating and cooling stage. The phase-transition temperatures and enthalpies were measured by carrying out DSC thermal analysis. The Cr, N, and I denote crystalline, nematic, and isotropic phases, respectively. The compound **7a** (Table 1) exhibited endothermic peaks with calculated enthalpy and entropy at 68.4°C ($\Delta H = 0.3$ kJ mol^{-1}) ($\Delta S = 0.9$ JK^{-1} mol^{-1}), 98.5°C ($\Delta H = 14.2$ kJ mol^{-1}) ($\Delta S = 38.2$ JK^{-1} mol^{-1}), 107.4°C ($\Delta H = 0.2$ kJ mol^{-1}) ($\Delta S = 2.3$ JK^{-1} mol^{-1}), 134.8°C ($\Delta H = 2.2$ kJ mol^{-1}) ($\Delta S = 5.4$ JK^{-1} mol^{-1}), 146.5°C ($\Delta H = 0.1$ kJ mol^{-1}) ($\Delta S = 0.3$ JK^{-1} mol^{-1}) and 186.7°C, which defines crystal-to-crystal polymorphic phases, and the peaks centered at 146.5°C and 186.7°C display nematic and isotropic phase transitions, respectively. The

Table 1. Transition temperatures (T) of the compound N-(4′-carboxybenzylidene)-4-n-alkoxybenzoyloxyaniline.

Compounds	Transition temperatures (°C)
7a	Cr$_1$ 68.4 (0.3)[a] (0.9)[b], Cr$_2$ 98.5 (14.2) (38.2), Cr$_3$ 107.4 (0.2) (2.3), Cr$_4$ 134.8 (2.2) (5.4) Cr$_5$ 146.5 (0.1) (0.3), N 186.7 (0.2) (0.5), I 184.3 (0.1) (0.3), N 144.3 (0.2)(0.5), Cr$_5$ 125.8 (2.4) (6.0), Cr$_4$ 104.6 (0.4) (1.1), Cr$_3$79.9 (13.8) (39.2), Cr
7b	Cr 134, N 153, I 146, N 121, Cr
7c	Cr 174, I 150, Cr
7d	Cr 120, I 118, N 98, Cr
7e	Cr 110, I 87, N 83, Cr
7f	Cr 240, I 99, Cr

[a] The value within the first set of parentheses denotes enthalpy in kJ mol^{-1}; [b] the value within the second set of parentheses denotes entropy in JK^{-1} mol^{-1}; Cr signifies crystal phase, N signifies nematic phase, and I signifies isotropic liquid.

exothermic peaks appear at 184.3°C ($\Delta H = 0.1$ kJ mol^{-1}) ($\Delta S = 0.3$ JK^{-1} mol^{-1}), 144.3°C ($\Delta H = 0.2$ kJ mol^{-1}) ($\Delta S = 0.5$ JK^{-1} mol^{-1}), 125.8°C ($\Delta H = 2.4$ kJ mol^{-1}) ($\Delta S = 6.0$ JK^{-1} mol^{-1}), 104.6°C ($\Delta H = 0.4$ kJ mol^{-1}) ($\Delta S = 1.1$ JK^{-1} mol^{-1}), and 79.9°C ($\Delta H = 13.8$ kJ mol^{-1}) ($\Delta S = 39.2$ JK^{-1} mol^{-1}), respectively, which defines isotropic-to-nematic phase transition followed by subsequent crystal phases. This compound displays enantiotropic nematic phase with the appearance of Schlieren texture as seen under optical microscopy. During the heating cycle at 146.5°C, the crystal phase transforms into radial bubbles, which sharply diminishes at the isotropic point. During the cooling cycle at 184.3°C, again the appearance of numerous radial bubbles or nematic droplets are seen, which enlarge and distribute as small patches showing striations embedded within the patches, giving the appearance of a very similar grandjean texture which is observed in the chiral nematic liquid crystals. The small patches showing striations or grooves and ridges embedded within the patches show a strong similarity with the "dermal plicae," which appears in the impression of the human fingerprint. However, it may be best compared with the grandjean texture of the chiral nematic mesophase.

The compound **7b** under optical microscopy displays nematic mesophase at 134°C during the heating cycle with the appearance of concentric radial nematic droplets occupying the full length of the vision area as seen under the optical microscope. The nematic droplets very slowly are seen to perish at the isotropization temperature of 153°C. During the cooling cycle at 146°C, nematic droplets with Schlieren texture are seen to appear. Within a larger droplet, numerous encircling bubbles with black stripes enclosed within the bubble cavity are seen, providing the evidence of the nematic mesophase. As the temperature further goes down to 121°C during the cooling cycle, a sharp transition toward the crystal phase is seen for this compound. Thus, this compound also displays enantiotropic mesophase with the appearance of nematic phase during both the heating and the cooling cycle.

The compounds **7d** and **7e** display a monotropic nematic phase as seen under optical microscope with the appearance of nematic phase at 118°C and 87°C during the cooling cycle only. During the heating cycle, both the compounds reach their isotropic temperature at 120°C and 110°C with no appearance of mesophase during the heating cycle. Thus, a sharp transition from crystal to isotropic phase was recorded for both the compound with prominent monotropic nematic mesophase with the appearance of characteristic textural pattern during the cooling cycle only. For both the compounds **7d** and **7e**, as seen individually under the optical microscope, the nematic droplets appear during the cooling cycle and get covered by the crystal phases at 98°C and 83°C, respectively.

The compounds **7c** and **7f** exhibited a sudden crystal-to-isotropic phase transition at 174°C and 240°C, respectively. During the cooling cycle, again isotropic-to-crystal phase transition are encountered at 150°C and 99°C, respectively, with no exhibition of mesophase during both the heating and the cooling cycle. Both these compounds were non-liquid crystalline, exhibiting a high isotropization temperature at 174°C and 240°C, respectively.

Thus, a structural–functional correlation is observed for the series of mentioned compounds **7a-7f** being analyzed for liquid crystallinity. The forces governing the liquid crystallinity in the series of mentioned compounds **7a-7f** are intermolecular interactions arising due to hydrogen bonding. These systems possess favorable intermolecular interactions via hydrogen bonding, which is responsible for generating the mesogenic behavior in this series of compounds.

The dimer state of the compound generated as a result of hydrogen bonding possesses the favorable intermolecular interaction responsible for generating the mesomorphic behavior. These intermolecular interactions have been tuned by the incorporation of aromatic rings and long alkoxy chains, which stabilize the mesomorphic properties. The compounds **7a**, **7b**, **7d**, and **7e** exhibited nematic mesophase, which is stabilized by the anisotropic van der Waal forces generated as a result of increasing alkoxy chain length. These anisotropic forces assist the hydrogen bonding forces, and as a result, the compounds display enantiotropic and monotropic nematic phase for the homolog with lower number of alkoxy chain length. But in higher members of the series with $m = 16$, the van der Waal forces overcome the hydrogen bond interaction, resulting in packing of the molecules and leading to the loss of mesomorphic behavior. Because the magnitudes of the dipole–dipole and dispersion forces that hold the thermotropic phases are critical, when they are too weak or too strong, the liquid crystalline character is lost. These forces being critical, ($m = 10$) (too low), do not bring the mesogenic nature in this compound. Being too low, these forces do not assist the intermolecular interaction generated as a result of hydrogen bonding.

Thus π–π dispersion forces from aromatic ring and intermolecular interactions as a result of hydrogen bonding favor the mesomorphic behavior, which is further assisted by anisotropic forces generated from the long alkoxy chain. In higher alkoxy chain length with $m = 16$, these forces are overcome by strong van der Waal forces resulting from the anisotropic alkoxy chain, which results in the loss of mesomorphic behavior.

5. Conclusions

A new series of mesomorphic acid dimers, N-(4′-carboxybenzylidene)-4-n-alkoxybenzoyloxyaniline, formed as a result of intermolecular hydrogen bonding having terminal alkoxy chains ($m = 6{\sim}16$) have been synthesized. The chemical structures of the final products were investigated by FTIR, UV-visible, ^{1}H, and ^{13}C NMR spectra. The existence of nematic phase was confirmed by optical microscopy. It was found that forces leading to the favorable molecular stacking as a result of hydrogen bonding results in acid dimers which exhibit mesomorphic properties. The prominent hydrogen bonding stabilizing the nematic mesophase is further suppressed by strong van der Waal forces originating from long alkoxy chain length with $m = 16$, which results in the loss of mesomorphic behavior in higher members of the series.

Acknowledgments

The authors thank the Head of the Department of Chemistry, Banaras Hindu University (BHU), Varanasi, India, for providing laboratory facilities. One of the authors (Ashwini Pandey) thanks the Council of Scientific and Industrial Research (CSIR, New Delhi, India) for financial support in the form of senior research fellowship at BHU. Thanks are also due to Mr. Satish Tiwari for CHN analyses, Mr. Shishir, Mr. Nagendra, and Mr. Amit for ^{1}H, ^{13}C NMR, and IR and electronic spectroscopy.

References

[1] Kato, T., & Frechet, J. M. J. (1989). *Macromolecules*, *22*, 3816.
[2] Kato, T., & Frechet, J. M. J. (1989). *J. Am. Chem. Soc.*, *111*, 8533.
[3] Kumar, U., Frechet, J. M. J., Kato, T., Ujhe, S., & Timura, K. (1992). *Angew. Chem. Int. Ed. Engl.*, *31*, 1531.
[4] Kumar, U., & Frechet, J. M. J. (1992). *Adv. Mater.*, *4*, 665.
[5] Bladdon, P., & Griffin, A. C. (1993). *Macromolecules*, *26*, 6604.
[6] Yu, L. J. (1993). *Liq. Cryst.*, *14*, 1303.
[7] Alexander, C., Jariwala, C. P., Lee, C. M., & Griffin, A. C. (1993). *Polym. Prep.*, *34*, 168.
[8] Kresse, H., Szulzewsky, I., Diele, S., & Paschke, R. (1994). *Mol. Cryst. Liq. Cryst.*, *238*, 13.
[9] Paleos, C. M., & Tsiourvas, D. (1995). *Angew. Chem. Int. Ed. Eng.*, *34*, 1696.
[10] Pourcain, C. B. S., & Griffin, A. C. (1995). *Macromolecules*, *28*, 4116.
[11] Schellhorn, M., & Lattermann, G. (1995). *Macromol. Chem. Phys.*, *196*, 211.
[12] Bernhardt, H., Weissflog, W., & Kresse, H. (1996). *Angew. Chem. Int. Ed. Engl.*, *35*, 874.
[13] Koh, K. N., Araki, K., Komori, T., & Shinkai, S. (1995). *Tetrahedron Lett.*, *36*, 5191.
[14] Kato, T., Hirota, N., Fujishma, A., & Frechet, J. M. J. (1996). *J. Polym. Sci. A. Polym. Chem.*, *34*, 57.
[15] Kato, T., Kihara, H., Ujhe, S., Uryu, T., & Frechet, J. M. J. (1996). *Macromolecules*, *29*, 8734.
[16] Price, D. J., Adams, H., & Bruce, D. W. (1996). *Liq. Cryst.*, *289*, 127.
[17] Kihara, H., Kato, T., Uryu, Y., Ujhe, S., Kumar, C., Frechet, J. M. J., Bruce, D. W., & Price D. J. (1996). *Liq. Cryst.*, *21*, 25.
[18] Kleppinger, R., Lillya, C. P., & Yang, C. (1997). *J. Am. Chem. Soc.*, *119*, 4097.
[19] Goldman, D., Dietel, R., Janietz, D., Schmidt, C., & Wendorff, J. H. (1998). *Liq. Cryst.*, *24*, 413.
[20] Yu, L. J., & Pan, J. S. (1993). *Liq. Cryst.*, *14*, 829.
[21] Paleos, C. M., & Tsiourvas, D. (2001). *Liq. Cryst.*, *28*, 1127.
[22] Gray, G. W., & Jones, B. (1954). "Molecular structures and properties of liquid crystals". *J. Chem. Soc.* 1467; Gray, G. W. (1962). In: *Molecular structure and Properties of Liquid Crystals*, Academic Press: London, p. 163 and references therein.
[23] Kelker, H., & Hatz, R. (1980). "Creation of liquid crystalline phases; A comparative view emphasizing structure and shape of monomer liquid crystals". In: *Hand Book of Liquid Crystals*, Verlag Chemie: Weinheim, p. 59.
[24] Kato, T., Kihara, H., Uryu, T., Ujie, S., Iimura, K., Frechet, J. M. J., & Kumar, U. (1993). *Ferroelecrtics*, *148*, 161.
[25] Kato, T., Uryu, T., Kaneuchi, F., Jin, C., & Frechet, J. M. J. (1993). *Liq. Cryst.*, *141*, 1311.
[26] Xu, B., & Swager, T. (1996). *J. Chem. Soc.*, *117*, 5011.
[27] Malik, S., Dhal, P. K., & Mashelkar, R. A. (1995). *Macromolecules*, *28*, 2519.
[28] Sideratou, Z., Tsiourvas, D., Paleos, C. M., & Skoulios, A. (1997). *Liq. Cryst.*, *22*, 51.
[29] Kato, T., Mizoshita, N., & Kishimoto, K. (2006). *Angew. Chem. Int. Ed.*, *45*, 38.
[30] Tschierske, C. (2001). *J. Mater. Chem.*, *11*, 2647.
[31] Briennem, M. J., Garad, J., Lehn, J.-M., & Stibor, I. (1989). *J. Chem. Soc. Commun.*, *11*, 1868.
[32] Fouquey, C., Lehn, J.-M., & Levelut, A. M. (1990). *Adv. Mater.*, *2*, 254.

[33] Goodby, J. W., Blinc, R., Clark, N. A., Lagerwall, S. T., Osipov, S. A., Pinkin, S. A., Sakurai, T., Yoshino, Y., & Zeks, B. (1991). "Ferroelectricity in liquid crystals and Polymers." Ed. G.W. Taylor. In: *Ferroelectric Liquid Crystals: Principles, Properties and Applications*, Gordon and Breach: Philadelphia, PA. p. 474.

[34] Clark, N. A., & Lagerwall, S. T. (1980). *Appl. Phys. Lett.*, *36*, 899.

[35] Fukuda, A., & Takezoe, H. (1990). In: *Structures and Properties of Ferroelectric Liquid Crystals*, (in Japanese) Corona: Tokyo, p. 355.

[36] Petrov, M. P., & Tsonev, L. V. (1996). *Liq. Cryst.*, *21*, 543.

[37] Kumar, P. A., Srinivasulu, M., & Pisipati, V. G. K. M. (1999). *Liq. Cryst.*, *26*, 859.

[38] Swathi, P., Kumar, P. A., & Pissipati, V. G. K. M. (2000). *Liq. Cryst.*, *27*, 665; Swathi, P., Kumar, P. A., & Pissipati, V. G. K. M. (2001). *Liq. Cryst.*, *28*, 1163–1169; Swathi, P., Kumar, P. A., & Pissipati, V. G. K. M. (2001). *Mol. Mater. 14*, 319; Swathi, P., Kumar, P. A., & Pissipati, V. G. K. M. (2001). *Z. Naturforsch 56a*, 103.

[39] Srinivasulu, M., Sattyanarayan, P. V. V., Kumar, P. A., & Pissipati, V. G. K. M. (2001). *Mol. Mater*, *14*, 215; Srinivasulu, M., Sattyanarayan, P. V. V., Kumar, P. A., & Pissipati, V. G. K. M. (2001). *Liq. Cryst*., *28*, 1321; Srinivasulu, M., Sattyanarayan, P. V. V., Kumar, P. A., & Pissipati, V. G. K. M. (2001). *Z. Naturforsch*, *56a*, 685.

[40] Swathi, P., Shastri, S. S., Kumar, P. A., & Pissipati, V. G. K. M. (2001). *Mol. Cryst. Liq. Cryst.*, *365*, 523.

[41] Singh, M. K. (2003). Synthesis and characterization of some mesogens and metallomesogens. PhD thesis, Banaras Hindu University, Varanasi, p. 54.

[42] Dave, J. S., & Vora, R. A. (1970). "Mesomorphic behaviour of the cholesteryl esters-I:p-n-alkoxybenzoates of cholesterol". In: J. F. Johnson & R. S. Porter (Eds.), *Liquid Crystals and Ordered Fluids*, Plenum: New York, p. 477.